Properties of General Relativistic Irrotational Binary Neutron Stars at the Innermost Orbit

Kōji Uryū[1*] and Masaru Shibata[2†]

[1] *Department of Physics, University of Wisconsin–Milwaukee, Milwaukee, USA*
[2] *Graduate School of Arts and Sciences, University of Tokyo, Komaba, Meguro, Tokyo, Japan*

Lecture given at the
Conference on Gravitational Waves:
A Challenge to Theoretical Astrophysics
Trieste, 5-9 June 2000

LNS013013

*uryu@uwm.edu
†shibata@provence.c.u-tokyo.ac.jp

Abstract

We investigate properties of binary neutron stars around innermost orbits, assuming that the binary is equal mass and in quasiequilibrium. The quasiequilibrium configurations are numerically computed assuming the existence of a helicoidal Killing vector, conformal flatness for spatial components of the metric, and irrotational velocity field for the neutron stars. The computation is performed for the polytropic equation of state with a wide range of the polytropic index n ($= 0.5, 0.66667, 0.8, 1, 1.25$), and compactness of neutron stars $(M/R)_\infty$ ($= 0.03-0.3$). Quasiequilibrium sequences of constant rest mass are appropriate models for the final evolution phase of binary neutron stars. It is found that these sequences are always terminated at the innermost orbit where a cusp (inner Lagrange point) appears at the inner edges of the stellar surface. We apply a turning point method to determine the stability of the innermost orbits and found that the innermost stable circular orbit (ISCO) exists for stiff equations of state ($n = 0.5$ with any $(M/R)_\infty$ and $n = 0.66667$ with $(M/R)_\infty \gtrsim 0.17$). The ISCO for $n = 0.5$ is carefully analyzed. It is clarified that the ISCO are mainly determined by a hydrodynamic instability for realistic compactness of the neutron stars as $0.14 \lesssim (M/R)_\infty \lesssim 0.2$. These configurations at the innermost orbits can be used as initial conditions for fully general relativistic simulation for the binary neutron star merger.

1 Introduction

The observations of binary neutron star systems such as Hulse Taylor pulser PSR1913 +16 [1] have revealed the existence of neutron star binary systems which will merge as a result of gravitational wave radiation reaction in the cosmological time $\sim 10^{10}$ yr. The last few minutes ($\sim$ 10000 cycles) of *inspiraling phase*, in which the characteristic orbital separation a is still much larger than the neutron star radius R ($a/R \gg 1$) and the orbital velocity v is much smaller than the speed of light c ($v/c \ll 1$), is a promising source of ground based laser interferometric detectors such as LIGO/VIRGO [2]. This phase can be treated by an analytic method using a post Newtonian approximation and equations of motion for point particles, resulting in recent successful developments ([3] see also, Will in this volume).

Great attention has been paid for subsequent *merger phase* of binary neutron stars. As a result of the merger, a black hole or a rapidly rotating supramassive neutron star will be formed. At this phase, the gravitational wave burst occurs on the merger process and quasi-periodic waves due to the ring down of the black hole quasi-normal mode or the oscillation of rapidly rotating supramassive neutron star will be emitted subsequently. These gravitational waves may be detectable by future narrow band gravitational wave detectors [4]. Also, the coalescence may be a source of high energy astrophysics phenomena, such as γ-ray burst [5] or r-process nuclei [6]. Numerical simulation of binary neutron star coalescence is the only way to investigate this phase. Therefore, intense effort has been made recently (see, for example, [7] and references therein).

In the *intermediate phase* between the inspiraling and the coalescing phase, the binary neutron stars still evolve in the adiabatic manner but a/R is the order of unity ($\sim 2-5$) that the effect of tidal deformation of neutron stars becomes important. In this phase, the binary neutron stars have to be treated numerically taking into account effects of the finite size, tidal deformation and hydrodynamic interaction. However, since the evolutional timescale is still longer than the dynamical timescale, we may assume quasiequilibrium circular orbits for the binaries. We focus on the intermediate phase in this article.

At the end of the intermediate phase, the binary neutron stars start coalescence from an innermost circular orbit. At this orbit, the gravitational wave signal could change abruptly from quasi-periodic waveform to burst waveform. In the frequency domain, such a change will be recognized as a clear cliff [8]. The characteristic frequency at the edge of the cliff may be used for extracting information about the nature of the equations of state (or the compactness) of high density neutron star matter, because the location of the innermost orbit depends sensitively on the equations of state of the neutron stars (see below). One of the main purposes of our calculation is to investigate the expected frequency for the innermost orbit, $f_{\rm GW}$, and to clarify the physical mechanism which determines the innermost orbits.

It is also important to locate the innermost orbit to prepare initial conditions for numerical simulations of merging binary neutron stars in full general relativity as well as to predict possible outcomes in simulations starting from such initial data sets. Several groups have been developing numerical codes for such simulation [9, 10, 11], and it is now feasible to perform the simulation stably and fairly accurately (see, [11] and Shibata in this volume). As indicated in [11], outcomes of the merger depend sensitively on the initial velocity field and compactness of the neutron stars. To obtain reliable results, we need to prepare the initial conditions as realistic as possible. The quasiequilibrium solutions of irrotational binary neutron stars near the innermost orbit provide appropriate initial conditions for the merger simulations.

Recently, we have computed solution sequences for binary neutron stars in quasiequilibrium from a distant configuration to an innermost configuration [12]. To approximate realistic stiff equations of state for the neutron stars, we adopt a polytropic equation of state in the form

$$P = \kappa \rho^{1+1/n} \tag{1}$$

where P, ρ, n and κ are the pressure, rest mass density, polytropic index, and polytropic constant, respectively. We can assume that the evolution in the intermediate phase is adiabatic (*i.e.*, κ is a constant), because the timescale for heating and cooling inside the neutron stars is much longer than the time spent in the intermediate phase. Since realistic equations of state for the neutron star matter are not yet clear [13], we choose a wide range for n between $n = 0.5$ and 1.25 to model various moderately stiff equations of state. We also survey a wide range of the compactness parameter $(M/R)_\infty$ from $(M/R)_\infty = 0.03$ to 0.3 where $(M/R)_\infty$ denotes the compactness of spherical neutron stars in isolation. With these parameter sets, we will be able to explore the effects of various realistic equations of state.

This article is organized as follows. We briefly review the formulation and numerical method in section 2, then we present numerical results and analyze the properties of irrotational binary neutron stars at the innermost orbits in section 3. We summarize the results in section 4. The geometrical unit $G = 1 = c$ are used throughout this paper. Greek indices run from 0 to 3 and Latin indices run from 1 to 3.

2 Formulation and solving method

The ratio of the radiation reaction timescale $\tau_{\rm GW}$ to the orbital period $\tau_{\rm rot}$ is evaluated using quadrupole formula and Newtonian expression of the energy as [14]

$$\frac{\tau_{\rm GW}}{\tau_{\rm rot}} \sim \frac{5}{128\pi}\left(\frac{a}{M_{\rm ADM}}\right)^{5/2} \simeq 1.1\left(\frac{a}{6M_{\rm ADM}}\right)^{5/2}, \tag{2}$$

where $M_{\rm ADM}$ is the ADM mass. This implies that even just before the merger at $a \gtrsim 6M_{\rm ADM}$, the reaction timescale is still longer than the orbital period and that the binary is approximately in a quasi stationary state. In this situation, we may assume the existence of a helicoidal Killing vector

$$\ell^\mu = \left(\frac{\partial}{\partial t}\right)^\mu + \Omega \left(\frac{\partial}{\partial \varphi}\right)^\mu. \tag{3}$$

We also assume that the velocity field of the neutron stars is irrotational. Viscosity inside the neutron stars is considered to be too weak to transport orbital angular momentum to spin on the emission timescale for gravitational waves [15]. If the spin period of the neutron stars is initially much longer than the final orbital period, the effect of the spin just before the merger is negligible. Therefore, the irrotational velocity field can be achieved. In this case, the relativistic Euler equation is integrated once [16]. Consequently, the procedure for obtaining a solution of the hydrodynamic equations is considerably simplified.

Assuming the spatial part γ_{ij} to be conformally flat [17, 18, 19], we write the metric in the 3+1 form,

$$ds^2 = g_{\mu\nu}dx^\mu dx^\nu = -(\alpha^2 - \beta_i\beta^i)dt^2 + 2\beta_i dx^i dt + \Psi^4 f_{ij}dx^i dx^j, \tag{4}$$

where α, β^i, Ψ and f_{ij} are the lapse function, shift vector, conformal factor, and flat spatial metric, respectively. The elliptic-type equations for α, β^i and Ψ are derived from the Hamiltonian constraint, momentum constraint and slicing condition $K_{ij}\gamma^{ij} = 0$ with the assumption $\gamma_{ij} = \Psi^4 f_{ij}$ as

$$\nabla^2\Psi = -\frac{1}{8}\Psi^{-7}\widetilde{K}_{ij}\widetilde{K}^{ij} - 2\pi\Psi^5\rho_H, \tag{5}$$

$$\nabla^2\beta^i + \frac{1}{3}\nabla^i\nabla_j\beta^j = -2\nabla_j\left(\alpha\Psi^{-6}\right)\widetilde{K}^{ij} - 16\pi\alpha\Psi^4 j^i, \tag{6}$$

$$\nabla^2\left(\alpha\Psi\right) = \alpha\Psi\left(\frac{7}{8}\Psi^{-8}\widetilde{K}_{ij}\widetilde{K}^{ij} + 2\pi\Psi^4(\rho_H + 2S)\right), \tag{7}$$

where ∇_i is the derivative with respect to the flat metric f_{ij} and K_{ij} is the extrinsic curvature. $\widetilde{K}^{ij}$ is defined as

$$\widetilde{K}^{ij} = \Psi^{10}K^{ij}, \tag{8}$$

$$\widetilde{K}^{ij} = -\frac{\Psi^6}{\alpha}\left(\frac{1}{2}\left(\nabla^i\beta^j + \nabla^j\beta^i\right) - \frac{1}{3}f^{ij}\nabla_k\beta^k\right). \tag{9}$$

The indices of $\widetilde{K}^{ij}$ are lowered by the flat metric f_{ij} as$\widetilde{K}_{ij} = f_{ik}f_{jl}\widetilde{K}^{kl}$. Fluid source terms in Eqs. (5), (6) and (7) are defined as

$$\rho_H = n^\mu n^\nu T_{\mu\nu}, \tag{10}$$

$$j^i = -\gamma^{i\,\mu} n^\nu T_{\mu\nu}, \tag{11}$$

$$S = \gamma^{ij} T_{ij}, \tag{12}$$

where n^μ is a unit normal of 3D spatial hypersurface. Note that $\gamma_{\mu\nu} = g_{\mu\nu} + n_\mu n_\nu$.

The energy momentum tensor $T_{\mu\nu}$ for a perfect fluid can be written as

$$T_{\mu\nu} = \rho \left(1 + \varepsilon + \frac{P}{\rho}\right) u_\mu u_\nu + P g_{\mu\nu}, \tag{13}$$

where ε and u_μ are the specific internal energy and the 4-velocity, respectively. We assume the polytropic equation of state as Eq. (1) and define the relativistic specific enthalpy h as

$$h = 1 + \varepsilon + \frac{P}{\rho} = 1 + \kappa\,(n+1)\,\rho^{1/n}, \tag{14}$$

where we use $\varepsilon = nP/\rho$.

Equations for the fluid are the first integral of Euler equation and the equation of rest mass conservation. For spatially conformal flat metric Eq. (4), they are written as follows.

$$\frac{h}{u^0} + h u_k \left(\frac{u^k}{u^0} - \Omega \xi^k\right) = \text{constant}, \tag{15}$$

$$\nabla_i \left(\rho\alpha\Psi^2 h^{-1} \nabla^i \Phi\right) = \nabla_i \left(\rho\alpha\Psi^6 h^{-1} (\omega^i + \Omega\xi^i)\right), \tag{16}$$

where, Φ is the velocity potential $h u_i = \nabla_i \Phi$, and ξ^i is a generator of rotation, $\xi^\mu = (0, -x^2, x^1, 0)$ in the Cartesian coordinates. The surface of the star is determined from

$$P = 0. \tag{17}$$

The boundary condition for the elliptic equation (16) is

$$\left(\frac{u^k}{u^0} - \Omega\xi^k\right) \nabla_i \rho \Big|_{\text{surf}} = 0. \tag{18}$$

Eqs. (16) and (18) form a system of elliptic type PDE with Neumann boundary condition.

We apply a second order finite difference scheme for the above equations. Those discretized equations are solved consistently by iteration. Numerical method and convergence tests are described in [19] in detail. We use spherical coordinates $(r_g, \theta_g, \varphi_g)$ to solve equations for the gravity Eqs.(5), (6) and (7), whose origin is at the center of mass of a binary system, and the surface fitted spherical coordinates $(r_f, \theta_f, \varphi_f)$ are used to solve equations for the fluid Eqs. (15) – (18). The typical number of coordinate grid points is listed in Table 1. We perform the Legendre expansion as Eq. (69) and Eq. (78) in the paper [19] and take the number of expansion up to $n_{\max} = 32$ and $l_{\max} = 10$ or 12, typically. We have checked the convergence of the numerical scheme and the effect of the truncation due to the Legendre expansion in [19]. These typical numbers for the grid points, $n_{\max}$ and $l_{\max}$ have been shown to give results with numerical errors being less than 0.5%.

$R_{g,\mathrm{mid}}/R_0$	$R_{g,\mathrm{max}}/R_0$	$N^r_{g,\mathrm{mid}}$	$N^r_{g,\mathrm{max}}$	N^θ_g	N^φ_g	N^r_f	N^θ_f	N^φ_f
5	100	80	20	40	60	16	16	32

Table 1: Parameters for the computational domains and the numbers of grid points in each coordinate system are listed. For $r_g \in [0, R_{g,\mathrm{mid}}]$, r_g coordinate grid is equidistant. For $r_g \in [R_{g,\mathrm{mid}}, R_{g,\mathrm{max}}]$, r_g coordinate grid is non-equidistant (logarithmic).

3 Result

3.1 Constructing solution sequences

We define the total rest mass $M_{0,\mathrm{tot}}$, ADM mass M_{ADM} and total angular momentum J_{tot} as

$$M_{0,\mathrm{tot}} = \int \rho\alpha u^0 \Psi^6 dV, \tag{19}$$

$$M_{\mathrm{ADM}} = \int \left[\rho h(\alpha u^0)^2 - P + \frac{1}{16\pi} K_{ij}K^{ij}\right] \Psi^5 dV, \tag{20}$$

$$J_{\mathrm{tot}} = \int \rho h \alpha u^0 u_\varphi \Psi^6 dV, \tag{21}$$

The integral is carried out over the whole three space. We also define the rest mass, gravitational mass and angular momentum per single neutron star as $M_0 = M_{0,\mathrm{tot}}/2$, $M = M_{\mathrm{ADM}}/2$ and $J = J_{\mathrm{tot}}/2$.

We define the coordinate length of the semi-major axis R_0 and half of orbital separation d as

$$R_0 = (R_{out} - R_{\mathrm{in}})/2, \tag{22}$$

$$d = (R_{out} + R_{in})/2, \tag{23}$$

where R_{in} and R_{out} denote distances from the center of mass of the system to the inner and outer edges of the star along the major axis, respectively. From these variables, we also define $\widehat{d} = d/R_0$. In the following, we adopt $\widehat{d}$ to specify a model along a quasiequilibrium sequence.

We also define half of the separation d_G in another way as

$$d_G = \frac{1}{M_{0,\mathrm{tot}}} \int |x| \rho\alpha u^0 \Psi^6 dV, \tag{24}$$

where x denotes a coordinate along the major axis. Hereafter, we often refer to d_G as the half of the orbital separation.

A quasiequilibrium sequence of irrotational binary neutron stars of the constant M_0 and κ with decreasing the orbital separation (or increasing Ω) can be identified as an evolutionary sequence of binary neutron stars as a result of gravitational

wave emission. Each sequence is computed gradually decreasing $\widehat{d}$ from 3 to 1. It is found that the sequences are always terminated at an innermost orbit with $\widehat{d} > 1$ and $d_G = d_R$ where the neutron stars have cusps at the inner edges of the stellar surfaces. This property is found irrespective of n and $(M/R)_\infty$. The cusps correspond to the inner Lagrange (L1) points.

To determine the dynamical stability of the binary orbits, we search for the minima of J and M as functions of the orbital separation (or the angular velocity) along each sequence. These minima of J and M should appear simultaneously at the same separation because the following identity likely holds for irrotational sequences in exact equilibrium with constant rest mass M_0;

$$dM_{\rm ADM} = \Omega dJ_{\rm tot}. \tag{25}$$

In our numerical computation, this identity is satisfied typically to $\lesssim 10\%$ except near to turning points where M and J are almost constant and consequently the difference between the neighborhoods is not accurately computed. Also, we checked that the minima of J and M appear simultaneously at the same d_G whenever they appear on a solution sequence. In view of this, we identify the location of the simultaneous minima of J and M as the ISCO.

In Fig. 1(a) and (b), we plot $J(d_G)$ for $n = 0.5$ and 0.66667, respectively, with $(M/R)_\infty = 0.19$. At the smallest separation in each panel, a cusp appears at the inner edge of the star. For $n = 0.5$, the minimum appears at $d_G > d_R$ as shown in Fig. 1(a), implying that the ISCO exist on the sequence. For $n = 0.66667$, the configuration at $d_G = d_R$ is almost marginally stable as shown in 1(b). We computed for $n = 0.5, 0.66667, 0.8, 1.0, 1.25$ with $(M/R)_\infty \lesssim 0.19$. It is found that the ISCO exists for $n = 0.5$ with any $(M/R)_\infty$ and for $n = 0.66667$ with $(M/R)_\infty \gtrsim 0.17$. On the other hand, for $n = 0.8, 1.0$ and 1.25 with $(M/R)_\infty \lesssim 0.19$, $J(d_G)$ does not have a minimum. Therefore, the innermost orbit, with a cusp at inner edge, is dynamically stable for these cases. At this innermost orbit, mass overflow likely starts prior to the onset of orbital instability.

The frequency of gravitational waves $f_{\rm GW}$ at the innermost orbit (which is the ISCO for $n = 0.5$, and 0.66667 with $(M/R)_\infty \gtrsim 0.17$, and is that of $d_G = d_R$ for the other cases) can be summarized as follows :

$$f_{\rm GW} \simeq \begin{cases} 0.8\left(\dfrac{1.5M_\odot}{M_0}\right)\text{kHz} & \text{for } (M/R)_\infty = 0.14, \\ 1.1 - 1.15\left(\dfrac{1.5M_\odot}{M_0}\right)\text{kHz} & \text{for } (M/R)_\infty = 0.17, \\ 1.35 - 1.4\left(\dfrac{1.5M_\odot}{M_0}\right)\text{kHz} & \text{for } (M/R)_\infty = 0.19. \end{cases} \tag{26}$$

$f_{\rm GW}$ does not depend strongly on n but on $(M/R)_\infty$. For a spherical neutron star with $M_0 \simeq 1.5M_\odot$ and $M_0 \simeq 1.4M_\odot$ in isolation, the radius will be in the range

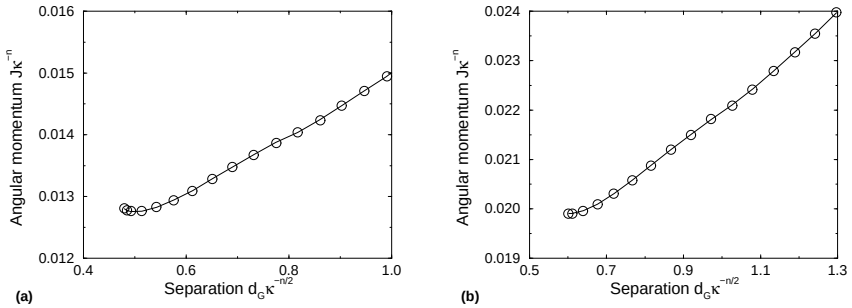

Figure 1: $\kappa^{-n} J$ is plotted as a function of $\kappa^{-n/2} d_G$ for (a) $n = 0.5$ and (b) $n = 0.66667$ with $(M/R)_\infty = 0.19$. The points of smallest d_G along the curves correspond to the configurations where the neutron stars have cusps at the inner edges of the stellar surfaces.

between 10 and 15km. This implies that $(M/R)_\infty$ is between $0.14 \lesssim (M/R)_\infty \lesssim 0.2$. The present result suggests that if the radius of neutron stars is fairly large, *i.e.*, $\sim$ 15km, the frequency of gravitational waves at the ISCO will be less than 1kHz which is in the sensitive frequency band of the laser interferometers such as LIGO/VIRGO. However, if the radius of neutron stars is ~ 10 km, the frequency at the ISCO is larger than 1kHz. The narrow band gravitational wave detector with a dual recycling technique or the resonant-mass detectors are required for the detection of the gravitational waves at the ISCO with $(M/R)_\infty \gtrsim 0.17$ [4].

3.2 Origin of the ISCO

The orbit of binary neutron stars can be destabilized either by the hydrodynamic (tidal) effect or by the general relativistic effect. To clarify which effect determines the ISCO for $n = 0.5$, we derive fitting formulas for $(M/R)_\infty < 0.2$ to see the dependence of $M_0\Omega$ and $M\Omega$ at the ISCOs on $(M/R)_\infty$. In the Newtonian limit $(M/R)_\infty \to 0$, $M_0\Omega(M/R)_\infty^{-3/2}$ and $M\Omega(M/R)_\infty^{-3/2}$ converge to an identical constant because they are non-dimensional and M_0 and M are identical in Newtonian gravity. The ISCO should be determined by the hydrodynamic effect in Newtonian limit as well as in the small but finite $(M/R)_\infty$ regime. Consequently, all of the general relativistic corrections should appear in the power series of $(M/R)_\infty$ from the viewpoint of the post Newtonian approximation. In view of these, we fix the functions of $M_0\Omega$ and $M\Omega$ in the form

$$M_0\Omega(M/R)_\infty^{-3/2} = a + b(M/R)_\infty + c(M/R)_\infty^2, \tag{27}$$

$$M\Omega(M/R)_\infty^{-3/2} = a' + b'(M/R)_\infty + c'(M/R)_\infty^2. \tag{28}$$

These coefficients are calculated by the least square fitting. We use the data set for $n = 0.5$ with $0.03 \leq (M/R)_\infty \leq 0.17$ (or 0.19) for the fitting.

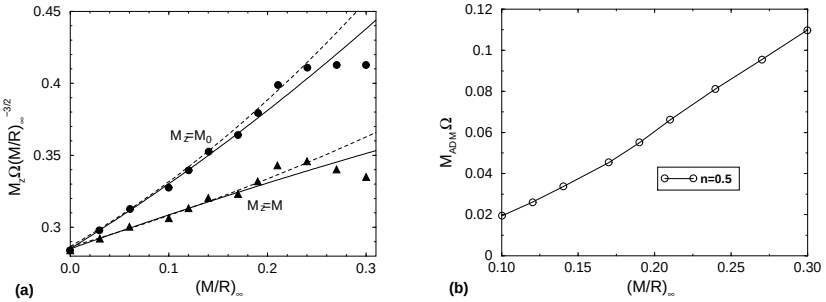

Figure 2: The plots of the angular velocity Ω at the ISCO as a function of compactness $(M/R)_\infty$ for $n = 0.5$ case. (a) The plot of $M_0\Omega(M/R)_\infty^{-3/2}$ (filled circles) and $M\Omega(M/R)_\infty^{-3/2}$ (filled triangles). The solid and dotted lines are the result of fitting formulas. The data sets with $0.03 \le (M/R)_\infty \le 0.17$ (solid lines) and $0.03 \le (M/R)_\infty \le 0.19$ (dotted lines) are used for each case. (b) $M_{\rm ADM}\Omega$ is plotted as a function of $(M/R)_\infty$.

In Fig. 2(a), $M_0\Omega(M/R)_\infty^{-3/2}$ and $M_{\rm ADM}\Omega(M/R)_\infty^{-3/2}$ at the ISCO are plotted as a function of $(M/R)_\infty$ together with the results from the fitting formulas derived above. The figure indicates that the numerical results are fitted fairly accurately in the form of Eqs. (27) and (28) for $(M/R)_\infty \lesssim 0.2$, which means that the post Newtonian expansion is appropriate in this regime.

The results of the fitting shows that the frequency of the ISCO depends strongly and systematically on $(M/R)_\infty$. Taking into account that the ISCO in the Newtonian limit is determined by the hydrodynamic instability, we may naturally infer that the ISCO for small $(M/R)_\infty \lesssim 0.2$ is still determined by the hydrodynamic instability with general relativistic corrections. Since the compactness of a realistic neutron star is likely to be in the range between $0.14 \lesssim (M/R)_\infty \lesssim 0.2$, the ISCO of the realistic binary neutron stars is determined by the hydrodynamic instability but not by the general relativistic instability. On the other hand, for $0.2 < (M/R)_\infty \le 0.3$, the fitting formulas do not agree with the numerical results, implying that the angular velocity at the ISCOs seems to be affected by strong nonlinear effects of general relativity. In this regime, the hydrodynamic effects seem to be less important.

In Fig. 2(b), we plot $M_{\rm ADM}\Omega$ at ISCOs as a function of $(M/R)_\infty$. It shows that $M_{\rm ADM}\Omega$ at the ISCOs increases with increasing $(M/R)_\infty$. As discussed above, the ISCO is determined by the hydrodynamic instability for $(M/R)_\infty \lesssim 0.2$. On the other hand, in the limit $(M/R)_\infty \to 1/2$, the hydrodynamic effects should become unimportant so that the general relativistic orbital instability can determine the ISCO. Cook [20] and recently Baumgarte [21] have investigated the ISCO for binary black holes using the conformal flat approximation for γ_{ij} as we did here. According to their results, $\mathcal{M}\Omega$ at the ISCO is 0.17–0.18. ($\mathcal{M}$ is the sum of the gravitational masses of the two black holes, and is slightly different from $M_{\rm ADM}$ although the

difference is not important here.) As shown in Fig. 2(b), $M_{\rm ADM}\Omega \simeq 0.11$ at the ISCO even at $(M/R)_\infty = 0.3$ and it is still monotonically increasing. This tendency does not contradict their results. We may expect that the ISCO of binary neutron stars is eventually determined by the general relativistic orbital instability for a sufficiently large $(M/R)_\infty > 0.3$ and $M_{\rm ADM}\Omega$ converges to a constant $\sim 0.17-0.18$, although such a large compactness is unrealistic for neutron stars.

Next, we compare the present results with those computed by the other methods. Kidder, Will and Wiseman [22], Damour, Iyer and Sathyaprakash [23], and Buonanno and Damour [24] have determined the ISCO using approximate relativistic equations of motion for two point particles in which some general relativistic corrections have been taken into account. They have derived the orbital angular velocity at the ISCO as $\mathcal{M}\Omega \simeq 0.0605$, 0.08850 and 0.07340, respectively. Since equations of motion for point particles have been used in their methods, the ISCO has been determined solely by the general relativistic orbital instability and $\mathcal{M}\Omega$ is independent of $(M/R)_\infty$.

Their results suggest that the point particle approximation can not be applied for binary neutron stars of $(M/R)_\infty \lesssim 0.2$. As we indicated above, the ISCO for $(M/R)_\infty \lesssim 0.2$ is likely to be determined by the hydrodynamic instability. In this range of $(M/R)_\infty$, $M_{\rm ADM}\Omega \lesssim 0.06$, which is smaller than their results. Namely, the orbits become unstable because of the hydrodynamic instability before the general relativistic effects between two stars become important. Since realistic neutron stars have $0.14 \lesssim (M/R)_\infty \lesssim 0.2$, the point particles approximation is not appropriate for investigating the ISCO of the binary neutron stars.

Our present results suggest that the ISCO may be determined by the hydrodynamic instability even for $0.2 < (M/R)_\infty \leq 0.3$ ($0.065 \leq M_{\rm ADM}\Omega \leq 0.11$), since $M_{\rm ADM}\Omega$ still depend on $(M/R)_\infty$ systematically. According to the point particle approximation, however, the general relativistic orbital instability should be important for $M_{\rm ADM}\Omega > 0.06 - 0.09$ implying that our results contradict theirs in this regime. The reason for this contradiction is not clear. The works of ourselves, Cook and Baumgarte are based on the conformal flatness approximation which may fail to include some important general relativistic effects that play an important role in determining the ISCO for the regime $(M/R)_\infty > 0.2$. To pin down the uncertainty for the high compactness regime, we need to carry out computations including higher general relativistic corrections.

4 Summary

We have investigated properties of innermost orbits of irrotational binary neutron star in quasiequilibrium assuming the polytropic equation of state. The quasiequilibrium sequences are calculated for wide parameter ranges of polytropic index $n = 0.5 - 1.25$ and the compactness $(M/R)_\infty = 0.03 - 0.3$.

The quasiequilibrium sequences for $n = 0.5$ with any $(M/R)_\infty$ and for $n = 0.66667$ with $(M/R)_\infty \gtrsim 0.17$ have a turning point which can be identified as the ISCO. For other parameters, ($n = 0.66667$ with $(M/R)_\infty \lesssim 0.17$ and $n \geq 0.8$), the sequences do not have the turning point even at the innermost configuration with a cusp (inner Lagrange points). For the former case, the binary orbit becomes unstable to start merging there. For the latter case, the mass overflow likely happens before the orbital instability sets in. The frequency of gravitational waves at these innermost orbits is between about 800 and 1500 Hz for $(M/R)_\infty \simeq 0.14 - 0.2$ depending on the compactness. For a binary of less massive (*i.e.*, less compact) neutron stars, the frequency is less than 1000 Hz. Therefore, the characteristic signal of gravitational waves emitted around the innermost orbit may be detected by laser interferometric detectors such as LIGO/VIRGO.

We investigate the physical origin the ISCO for $n = 0.5$ using fitting formulas. The results indicate that the ISCO is determined not by the general relativistic instability, but by the hydrodynamic instability for the parameter range of realistic binary neutron stars, $0.14 \lesssim (M/R)_\infty \lesssim 0.2$. This implies that point particle approximations are not appropriate for determining the ISCO of binary neutron stars as long as the neutron stars are not extremely compact $(M/R)_\infty \gg 0.2$.

In our formulation, the Hamiltonian and momentum constraints are solved consistently, and hence these quasiequilibrium states of irrotational binary neutron stars at the innermost orbits can be used as initial conditions for the fully general relativistic simulations of binary merger. Such simulations have recently been performed in [11] (see also Shibata in this volume) and further detailed analysis for the initial configurations at the innermost orbits as we discussed in this article will be found in another paper [12].

Acknowledgments

We thank John C. Miller, Yoshiharu Eriguchi and Luciano Rezzolla for discussions and continuous encouragement. We also thank Dennis W. Sciama for his warm hospitality at SISSA. A part of numerical computations was performed at the data processing center of National Observatory of Japan.

References

[1] R.A. Hulse and J.H. Taylor, Astrophys. J. **195**, L51 (1975); J.H. Taylor, L.A. Fowler and P.M. McCulloch, Nature **277**, 437 (1979).

[2] A. Abramovici et al. Science **256**, 325 (1992) ; C. Bradaschia, et al. Nucl. Instrum. and Methods **A289**, 518 (1990).

[3] e.g., L. Blanchet, Prog. Theor. Phys. Suppl. **136**, 146 (1999) ; C. M. Will, Prog. Theor. Phys. Suppl. **136**, 158 (1999).

[4] C. Cutler et al., Phys. Rev. Lett. **70**, 2984 (1993),

[5] e.g., T. Piran, in *Unsolved Problems in Astrophysics*, edited by J. N. Bahcall and J. P. Ostriker (Princeton University Press, 1997), 343.

[6] C. Freiburghaus, S. Rosswog and F.-K. Thielemann, Astrophys. J. Lett. **525**, L121 (1999).

[7] K. Oohara, T. Nakamura and M. Shibata, Prog. Theor. Phys. Suppl. **128**, 183 (1997).

[8] X. Zhuge, J. M. Centrella, and S. L. W. McMillan, Phys. Rev. D **50**, 6247 (1994).

[9] K. Oohara and T. Nakamura, Prog. Theor. Phys. Suppl. **136**, 270 (1999); J. A. Font, M. Miller, W.-M. Suen, and M. Tobias, Phys. Rev. D **61**, 044011 (2000); W.-M. Suen, Prog. Theor. Phys. Suppl. **136**, 251 (1999); W. Landry and S. A. Teukolsky, preprint gr-qc/9912004 (1999).

[10] M. Shibata, Prog. Theor. Phys. **101**, 251 (1999); M. Shibata, Prog. Theor. Phys. **101**, 1199 (1999); M. Shibata, Phys. Rev. D **60**, 104052 (1999).

[11] M. Shibata and K. Uryū, Phys. Rev. D **61**, 064001 (2000).

[12] K. Uryū, M. Shibata and Y. Eriguchi, Phys. Rev. D in press.

[13] e.g., H. Heiselberg and M. Hjorth-Jensen, Phys.Rept. **328**, 237 (2000).

[14] e.g., S. L. Shapiro and S. A. Teukolsky, *Black Holes, White Dwarfs and Neutron Stars*, (Wiley, New York, 1983).

[15] C. S. Kochanek, Astrophys. J. **398**, 234 (1992); L. Bildsten and C. Cutler, Astrophys. J. **400**, 175 (1992).

[16] S. Bonazzola, E. Gourgoulhon and J.-A. Marck, Phys. Rev. D **56**; 7740 (1997); H. Asada, Phys. Rev. D **57**, 7292 (1998); M. Shibata, Phys. Rev. D **58**, 024012 (1998); S. A. Teukolsky, Astrophys. J. **504**, 442 (1998).

[17] J. R. Wilson and G. J. Mathews, Phys. Rev. Lett. **75**, 4161 (1995); P. Marronetti, G. J. Mathews and J. R. Wilson, in the proceedings of 19th Texas Symposium on Relativistic Astrophysics: Texas in Paris, Paris, France (1998); P. Marronetti, G. J. Mathews and J. R. Wilson, Phys. Rev. D **60**, 087301 (1999).

[18] S. Bonazzola, E. Gourgoulhon and J.-A. Marck, in the proceedings of 19th Texas Symposium on Relativistic Astrophysics: Texas in Paris, Paris, France (1998); S. Bonazzola, E. Gourgoulhon and J.-A. Marck, Phys. Rev. Lett. **82**, 892 (1999).

[19] K. Uryū and Y. Eriguchi, Phys. Rev. D. **61**, 124023 (2000).

[20] G. B. Cook, Phys. Rev. D **50**, 5025 (1994).

[21] T. W. Baumgarte, Phys.Rev. D **62**, 024018 (2000).

[22] L. E. Kidder, C. M. Will, A. G. Wiseman, Phys. Rev. D **47**, 3281 (1993).

[23] T. Damour, B. R. Iyer, B. S. Sathyaprakash, Phys. Rev. D **57**, 885 (1998).

[24] A. Buonanno, T. Damour, Phys. Rev. D **59**, 084006 (1999).